

ICRR 313-94-8
SU 9415
ICRR-Report-313-94-8
TITHE-94-2

55

**Observation of 7 TeV Gamma Rays
from the Crab using the Large Zenith Angle
Air Čerenkov Imaging Technique**

T. Tanimori, T. Tsukagoshi, T. Kifune, P. G. Edwards, M. Fujimoto,
T. Hara, N. Hayashida, Y. Matsubara, Y. Mizumoto, Y. Muraki,
S. Ogio, J. R. Patterson, M. D. Roberts, G. P. Rowell, T. Suda,
T. Tamura, M. Teshima, G. J. Thornton, Y. Watase, and T. Yoshikoshi



(March, 1994)

*Submitted for publication in
Astrophysical Journal Letters*

3-2-1 Midori-cho Tanashi, Tokyo 188 Japan

Telephone (0424)-61-4131, Telefax (0424)-68-1438

Observation of 7 TeV Gamma Rays from the Crab using the Large Zenith Angle Air Čerenkov Imaging Technique

T.Tanimori⁽¹⁾, T.Tsukagoshi⁽¹⁾, T.Kifune⁽²⁾, P.G.Edwards⁽³⁾, M.Fujimoto⁽⁷⁾,
T.Hara⁽⁸⁾, N.Hayashida⁽²⁾, Y.Matsubara⁽⁵⁾, Y.Mizumoto⁽⁴⁾, Y.Muraki⁽⁵⁾,
S.Ogjo⁽¹⁾, J.R.Patterson⁽³⁾, M.D.Roberts⁽³⁾, G.P.Rowell⁽³⁾, T.Suda^{(4)*},
T.Tamura⁽²⁾, M.Teshima⁽²⁾, G.J.Thornton⁽³⁾, Y.Watase⁽⁶⁾, and T.Yoshikoshi⁽¹⁾

- (1)Department of Physics, Tokyo Institute of Technology, Tokyo 152, Japan
(2)Institute for Cosmic Ray Research, University of Tokyo, Tokyo 188, Japan
(3)Department of Physics and Mathematical Physics, University of Adelaide, South Australia 5005, Australia
(4)Department of Physics, Kobe University, Hyogo 637, Japan
(5)Solar Terrestrial Environment Laboratory, Nagoya University, Nagoya 464, Japan
(6)National Laboratory for High Energy Physics, Ibaraki 305, Japan
(7)National Astronomical Observatory, Tokyo 181, Japan
(8)Department of Information Technology, Yuge National College of Maritime Technology, Ehime 794-25, Japan
* deceased

Abstract

We have observed the Crab pulsar/nebula from 1992 December to 1993 January to search for very high energy gamma rays, using an imaging air Čerenkov telescope of 3.8m diameter, located at Woomera, Australia. Since the observation was carried out in the southern hemisphere, the zenith angle of the object is large, which results in a maximum sensitivity of $\sim 10^{-13}\text{cm}^{-2}\text{s}^{-1}$ with ~ 7 TeV threshold energy for detected gamma rays. With high angular resolution, the Čerenkov imaging technique is found to be useful at zenith angles 53° – 56° . We report here possible evidence of detection with 4σ significance of very high energy gamma-rays above ~ 7 TeV from the Crab pulsar/nebula. The integral flux is estimated to be $(7.6\pm 1.9)\times 10^{-13}\text{cm}^{-2}\text{s}^{-1}$. The result is consistent with the revised spectrum of the Crab recently reported by the Whipple group (Lewis et al. 1993).

Subject Headings: gamma rays:observations – nebulae:Crab Nebula – pulsars

1. Introduction

It has been known for many years that relativistic electrons are accelerated in the Crab pulsar/nebula and non-thermal radiation is emitted in a wide band of wavelengths, making it the best studied galactic object in various wavelength regions. Attempts to detect very high and ultra high energy γ -rays have continued for almost 30 years with ground-based detectors. The highest energy at which the source has so far been detected with sound statistics is in TeV γ -rays with the imaging Čerenkov telescope of the Whipple group (Weekes et al. 1989; Vacanti et al. 1991). Following this detection of $\sim 25\sigma$ significance, repeated on many occasions, the Themistocle group in France reported a positive detection in the higher energy region of 3 - 15 TeV (Baillon et al. 1993) also with Čerenkov telescopes, not of imaging capability but having a reasonably good angular resolution of $\sim 0.1^\circ$ because of fast timing characteristics. Beyond 10 TeV a number of efforts have been and are being made with air shower arrays (Amenomori et al. 1992; Alexandreas et al. 1991; Cronin et al. 1992).

Knowledge of the Crab energy spectrum at these high energies is important to clarify the high energy limit of particle acceleration. Satellite-borne detectors, most recently and notably the EGRET detector of the Compton Gamma Ray Observatory (Nolan et al. 1993; De Jager et al. 1993), have determined the pulsed and unpulsed energy spectrum from the Crab in the energy region from 100 MeV to 10 GeV. The high energy radiation from the Crab pulsar/nebula is explained by synchrotron radiation from TeV electrons and inverse Compton emission at higher energies. The Whipple result indicates that unpulsed emission becomes dominant from 300 GeV to a few TeV energies. The TeV flux is considerably lower than the extrapolation of the pulsed GeV spectrum detected with EGRET, but is larger than the extrapolation from GeV unpulsed one, suggesting some acceleration mechanism of electrons and positrons in the nebula region (De Jager & Harding 1992). Knowledge of the energy spectrum in the TeV energy region or even higher is necessary to further uncover what takes place in the pulsar/nebula, and to examine the self consistency between the two processes, synchrotron and inverse Compton emission, and to know the fate of the most energetic electrons.

The Crab is not the only pulsar which emits GeV and possibly TeV γ -rays. Four more young pulsars have been found to emit such energetic γ -rays (Vela pulsar, Thompson et al. 1975; Geminga, Bertsch et al. 1992; PSR1706-44, Thompson et al. 1992; PSR1055-52, Fierro et al. 1993). A comparison of energy spectra from these pulsars would also be necessary to understand the high energy processes which take place.

However, the Crab is still unique as a standard candle for calibrating ground-based detectors of very high energy γ -rays.

There is presently a discrepancy between the Whipple and Themistocle energy spectra of the Crab (Lewis et al 1993; Baillon et al 1993). The present paper reports a result at ~ 7 TeV which was obtained with an imaging Čerenkov telescope. The comparison of this result with those of the Whipple and Themistocle groups is particularly useful for calibrating our telescope, which is located in the southern hemisphere where we have an advantage of observing three other γ -ray pulsars: the Vela pulsar, PSR1706-44, and PSR1055-52, near the zenith.

We have observed the Crab region near its culmination at zenith angle 53° . Sommers and Elbert (1987) pointed out that Čerenkov telescopes have a larger collecting area at large zenith angles and a higher threshold energy. The resulting detection area is as large as 10^9 cm^2 , which enables us, with 10^5 s observation time, to detect a γ -ray flux of the order of $10^{-13} \text{ cm}^{-2} \text{ s}^{-1}$. This sensitivity is currently the best among various types of detectors above a threshold energy of several TeV.

2. Instrumentation

The observation was made with the 3.8m telescope of the CANGAROO collaboration between Japan and Australia (Patterson and Kifune 1992), which allows for very high energy γ -ray stereoscopic observation with two Čerenkov imaging telescopes from the both sides of the collaboration, although stereo data is not presented here. The 3.8m telescope (Hara et al. 1992) is located at Woomera in South Australia ($136^\circ 47'$ E and $31^\circ 06'$ S), and installed at 100m east of the BIGRAT telescope of University of Adelaide. The telescope is on an alt-azimuth mount, and has a parabolic mirror with a 3.8m diameter and 3.8m focal length. The focus of the telescope has an image plane point spread function of about 0.01° , better than other contemporary Čerenkov telescopes.

The camera consists of small square-shaped photomultiplier tubes $10\text{mm} \times 10\text{mm}$ size (Hamamatsu R2248). The number of photomultipliers is 220, giving a total field of view of about 3° in diameter. Eight photomultipliers are installed in one module with a common high voltage generator, bleeder resistors for photomultipliers, and buffer amplifiers to feed signals through 30m-long twisted pair cables. The photocathode of each photomultiplier covers an area of $8\text{mm} \times 8\text{mm}$, corresponding to $0.12^\circ \times 0.12^\circ$.

The photo-sensitive area of the camera is estimated to cover $\sim 40\%$ of the total field of view. The relative-gain of each photomultiplier were calibrated by using a fast-risetime LED (light emitting diode) driven with a fast pulse of 20nsec width. In order to avoid saturation currents due to bright stars within the field of view, photomultipliers were operated with a gain of $\sim 10^5$. A buffer and a main amplifier in the front-end electronics compensate for the

relatively low gain in the photomultiplier tubes. The high voltage on all the phototubes can be kept turned on when a magnitude 3 star enters a field of view.

By detecting the passage across the phototubes of a bright star in the field of view, both the direction of telescope pointing and the aperture of the camera was calibrated. When observing the Crab region, ζ Tau, a star of magnitude 3.0, is located at a distance of 1.1° from the center of the field of view. The tracking accuracy was estimated to be within $\pm 0.1^\circ$, about a half of the photomultiplier size.

In order to process the output pulse from photomultiplier tubes, we developed a circuit module, known as a CCM (Čerenkov Circuit Module). Each of these modules has 16 inputs and contains high gain amplifiers ($\times 100$), discriminators, TDC (time to digital converter), ADC (analog to digital converter), scalars, dc current monitors, and summing circuits for obtaining both the number of photomultipliers "hit" and the total pulse height. A high resolution TDC ($\delta t \sim 0.25\text{ns}$) is used for each channel to measure the arrival time of photons in each phototube. In the CCM circuit, the output from each photomultiplier is also fed to an ADC. The amplified pulse is discriminated at a common preset value which corresponds to ~ 3 photoelectrons for each photomultiplier. The discriminated pulse is then used (1) for stopping the TDC count which has been started by the event trigger. (2) for monitoring the gain and the stability of each photomultiplier by counting the number of the discriminated pulses during 1 ms (which is recorded at every event trigger), and (3) for summing with those in the other channels (called the "Hit Sum"). In addition, input pulses, without discrimination, are added together to form a "Linear Sum". These two summed outputs are further added over all CCM circuits, and then used to generate the trigger pulse for recording data. When a trigger occurs, the data processed by the CCM are transferred to an on-board micro processor, 68020, through a CAMAC memory module in which the real timing operating system, OS9, is used.

A trigger pulse is generated when the Linear Sum (the total amount of light received by the camera) is larger than ~ 10 photoelectrons, and at the same time the Hit Sum (the number of photomultipliers having a signal above the discriminator level) exceeds a preset number (~ 3 -hits).

3. Analysis and Result

The Crab pulsar/nebula was observed at zenith angles of $53^\circ - 56^\circ$ between 1992 December 19 and 1993 January 27. The observation time is 1.6×10^5 second and 0.93×10^5 second for on- and off-source runs of the Crab region observation, respectively. At such large zenith

angles, both the threshold energy and the effective area of detection increase by a factor of ~ 7 compared with viewing at the zenith.

For each event, the imaging parameters were calculated from the raw data as described by Weekes et al. (1989). These parameters can be classified into three types, (1) those related to the elongated shape of the Čerenkov light image such as “width” and “length”, (2) “conc” which is the fraction of the total light yield concentrated into three photomultipliers, and (3) those describing the image location on the camera plane such as “distance” (the distance between the centroid of the image and the center of the field of view) and the orientation angle α of the image.

The parameter α is defined as the angle between the major axis of an ellipse fitted to the image of each event and a line connecting the center position of the field of view with the centroid of the image. The distribution of angle α is expected to appear as a peak near 0° when an event is due to a γ -ray from a point source usually set at the center of field of view. Cosmic ray images have a flat distribution in α . The peak is sensitive to pointing errors of an object at the center of the field of view so that the position of γ -ray point source is determined with an accuracy of $\sim 0.1^\circ$. Parameters of type (1) and (2) take dissimilar values depending on whether the event is caused by a γ -ray or a cosmic ray proton; namely the “width” of γ -ray events is smaller than that of cosmic rays, and “conc” is larger. Thus, the selection of narrower “width” and larger “conc” can enrich γ -ray events.

The large zenith angles, however, cause a shrinkage of the Čerenkov light image. The light intensity is more concentrated in a smaller and narrower angular region than for observations near the zenith. The imaging parameters “width” and “length” tend to become smaller, and “conc” tends to get larger. Thus, in the case of the present observation at large zenith angles, we have to be careful about these effects, and we have used cuts as loose as possible to avoid over-cutting γ -ray events.

In the first stage of the data analysis the false events, which were caused by accidental coincidences due to background light of the night sky or from electrical noise, were rejected by requiring that the arrival times of Čerenkov photons hitting each photomultiplier tube should be within ~ 50 nsec. We then selected the events of good quality in which at least 4 photomultipliers are hit by Čerenkov photons and the Linear Sum is more than 15 photoelectrons. The events with “distance” larger than 0.9° or smaller than 0.16° were excluded, since the images of these events are located either along the outer boundary or very near the center of the field of view. In the latter case, α is less accurately determined because the image becomes nearly circular.

Figure 1a shows the α distributions for both on- and off-source events passing the above cuts. Note that a peak appears around 0° even for the data set of on-source events while such

a peak is not seen for off-source events, even though no cuts which specifically select against hadron showers have been applied. In the next stage of analysis, the events having “width” larger than 0.14° or “length” larger than 0.33° were removed, in order to enrich γ -ray events in the data sample. In addition, the events with “conc” smaller than 0.4 were excluded. The energy dependence of these cuts was taken into account in the analysis. The resulting event rate is plotted in Figure 1b as a function of α . A peak of events is seen at α around 0° in the on-source data, but not in the off-source data set. About 90% of the excess events in Figure 1a having $\alpha < 15^\circ$ remained after the cut to obtain Figure 1b from Figure 1a, while a half of the events of larger α values did not satisfy the selection criteria.

In order to evaluate our method of analysing the Čerenkov image, the imaging parameters calculated from the data were compared with the result of a Monte Carlo simulation which was generated using the code GEANT 3.15 (Brun et al. 1984; Fesefeldt 1985). The distributions of simulated “width” and “length” are shown in Figure 2 for hadron events. The image parameters of the experimental data show a distribution similar to those of hadron showers, since more than 99% of the data must be from cosmic ray particles such as protons. The observed distribution is consistent with the simulation result, although better statistics for simulated events would be desirable. The shower particles which can emit Čerenkov light were fully traced in the simulation.

Effects due to the bright star, which is located at 1.1° from the Crab pulsar/nebula and within the field of view of the camera, were examined. The location of Čerenkov image was examined in the image plane, and we found that the centroid of the image distributed uniformly not correlated with ζ tau position. No effect was found that could cause a peak at 0° as observed.

The events contributing to a peak at $\alpha \sim 0^\circ$ are from the full range of the observed values of the total yield of Čerenkov photons, which is considered to be in proportion to the energy of γ -rays. It is thus evident that this peak in the α distribution is not due to a spurious effect which may appear near the limit of detector sensitivity.

4. Discussion

When we attribute the peak in the α distribution to γ -rays from the Crab pulsar/nebula, and subtract the flat distribution of the background estimated from α in the range 15° – 90° , the excess counts of γ -ray events within the bins of $\alpha < 15^\circ$ in Figure 1b has a statistical significance of 4σ . When we take a conservative view of estimating the statistical significance only from the counting rate of $\alpha < 15^\circ$, the formula given by Li and Ma (1983) gives 3σ for the data in Figure 1b. The width of the observed α peak in this figure is consistent with

the result of Monte Carlo simulation which took into account the uncertainties coming from possible misalignments in the phototube camera and from effects due to the environmental night sky background light.

The detection area and threshold energy of the detector for a γ -ray shower were inferred from the Monte Carlo simulation. The threshold energy for detecting a γ -ray shower was also estimated to be ~ 7 TeV, provided that the power index of the differential energy spectrum of γ -ray from the Crab pulsar/nebula is near -2.7 , as reported by the Whipple group. The light pool of Čerenkov photons emitted from a γ -ray shower is known to have a uniform intensity at sea level over a few hundred meters around the shower axis. However, the radius of the light pool varies with the zenith angle of the shower arrival direction. At zenith angles of 53° – 56° , the averaged radius of the Čerenkov light pool was estimated to be 320m for 7 TeV γ -ray showers, which corresponds to a detection area of $3.2 \times 10^9 \text{cm}^2$. Based on the observation time of 28.5 hours, the excess events attributed to γ -rays from the Crab pulsar/nebula is $2.7 \cdot \xi^{-1} \cdot \eta^{-1} \times 10^{-13} \text{cm}^{-2} \text{s}^{-1}$, where ξ is the combined efficiency for triggering and identifying the shower events in the analysis at ~ 7 TeV, and η is the efficiency of γ -ray events passing through the data reduction procedures for the enrichment of γ -ray events, respectively. The efficiency ξ was estimated to be 0.41 from the Monte Carlo simulation, and η was 0.87 from the surviving fraction of the events in the peak at ~ 0 degree after the cuts obtaining Figure 1b from Figure 1a. These values are consistent with the Monte Carlo simulation. The flux of γ -rays with energy greater than ~ 7 TeV is, thus, calculated to be $(7.6 \pm 1.9) \times 10^{-13} \text{cm}^{-2} \text{s}^{-1}$.

In this procedure, the largest uncertainty exists in estimating the threshold energy which depends on various parameters such as the reflectivity of the mirror, energy spectrum of γ -rays and the sky conditions. The estimation of detection area is on the other hand considered to be more reliable. The systematic error was evaluated from the uncertainties of the power index of energy spectrum, the trigger conditions, and the reflectivity of the mirror. Each term was quadratically added yielding $\pm \sim 1.5$ TeV as the total.

Recently the Whipple group has revised the analysis of their data from the 1988/1989 observation, resulting in a change of the index of the differential energy spectrum from -2.4 ± 0.3 to $-2.69 \pm 0.09 \pm 0.3$ (Lewis et al. 1993). Recent results on γ -rays around 7 TeV from the Crab pulsar/nebula are presented in Figure 3. As shown in Figure 3, the integral flux of γ -rays calculated from the new Whipple's differential energy spectrum leads to an apparent discrepancy with the Themistocle data above ~ 3 TeV (Baillon et al. 1993). Although the statistics of the revised Whipple energy spectrum above 3 TeV are poor, with a significance of $\sim 2\sigma$, a smooth continuation from the Whipple energy spectrum below 3 TeV seems difficult to explain the Themistocle data at higher energies. The present data point near 7

TeV is within the uncertainty of the Whipple intensity, and outside the uncertainty of the Themistocle data. It constrains the allowed energy spectrum above ~ 7 TeV.

It is likely that we have observed γ -rays from the Crab pulsar/nebula at ~ 7 TeV energy with a significance of 4σ , though the significance is marginal. The result was obtained by applying the Čerenkov imaging technique to large zenith angle observation. It demonstrates that the method of Čerenkov light imaging at large zenith angles provides a high sensitivity of $\sim 10^{-13} \text{cm}^{-2} \text{s}^{-1}$ in the energy region of ~ 7 TeV and that the high resolution camera of the 3.8m telescope is capable of enriching γ -rays and determining the source location with an accuracy of $\sim 0.1^\circ$.

This work is supported by a Grant-in-Aid in Scientific Research of the Japan Ministry of Education, Science and Culture, and also by the Australian Research Council and International Science and Technology Program.

REFERENCES

- Alexandreas, D. E., et al. 1991, ApJ, 383, 653
- Amenomori, M., et al. 1992, Phys. Rev. Lett., 69,2468
- Baillon, P., et al. 1993, Proc. 23rd Internat. Cosmic Ray Conf.(Calgary),1, 271
- Bertsch, D. L., et al. 1992, Nature, 357, 306 Brun, R., Bruyant, F., Maire, M., McPherson, A. C., & Zanarini, P. 1984, *CERN/DD/EE/84-1* (Geneva: CERN), 1987
- Cronin, J. W., et al. 1992, Phys. Rev., D45, 4385
- De Jager, O. C., & Harding, A.K. 1992, ApJ, 396, 161
- De Jager, O. C., et al. 1993, IAU Circular No. 5887
- Fesefeldt, H. 1985, *PreprintPITHA85/02* Aachen
- Fierro, J. M., et al. 1993, ApJ, 413, L27
- Hara, T., et al. 1993, Nucl. Instr. and Meth., A332, 300
- Li, T. P., & Ma, Y. Q. 1983, ApJ, 272, 317
- Lewis, D. A., et al. 1993, Proc. 23rd Internat. Cosmic Ray Conf.(Calgary),1, 279
- Nolan, P. L., et al. 1993, ApJ, 409, 697
- Patterson, J. R., & Kifune, T. 1992, Australian and New Zealand Physicist 29, 58
- Sommers, P., & Elbert, J. W., 1987, J.Phys. G:Nucl. Phys., 13, 553
- Thompson, D. J., et al. 1975, ApJ, 200, L79
- Thompson, D. J., et al. 1992, Nature, 359, 615
- Vacanti, G., et al. 1991, ApJ, 377, 467
- Weekes, T. C., et al. 1989, ApJ, 342, 379

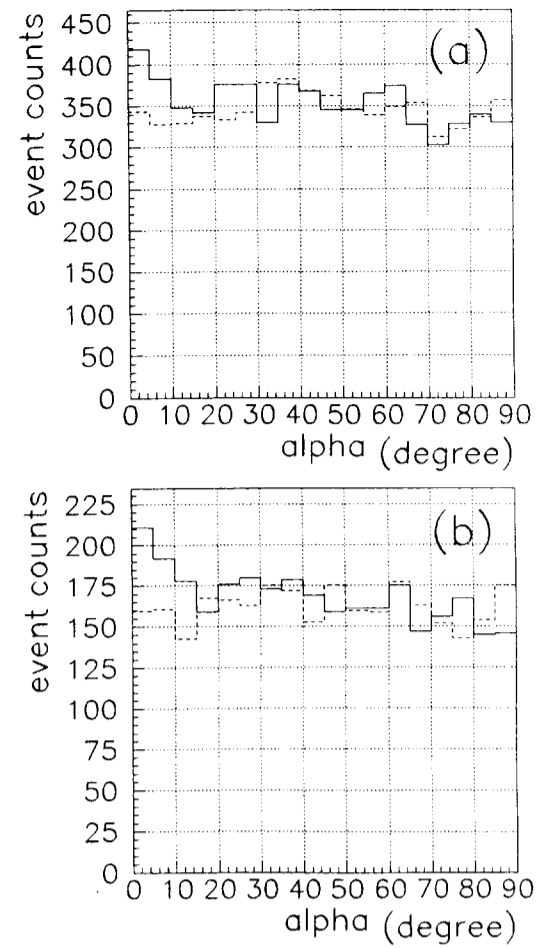


Figure 1: (a): The α distributions both for on- (solid line) and off source (dashed line) events passing through the requirements of ≥ 4 hits of phototubes and the total amount of ≥ 15 photoelectrons. (b): The α distributions for the final data which survived after the γ -ray event selection. See text for the details.

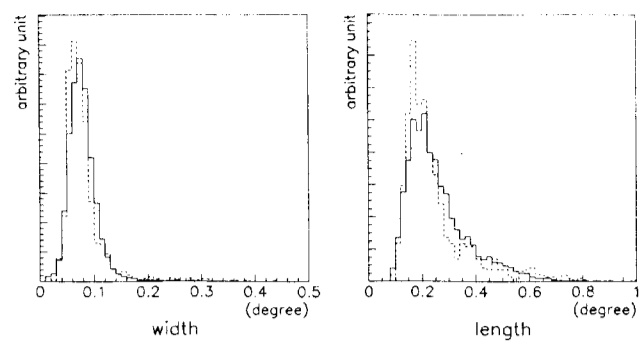


Figure 2: The comparisons between simulated and measured events of imaging parameters, width and length, where the distributions of the real data are shown as solid lines, and those of the simulation as dashed lines.

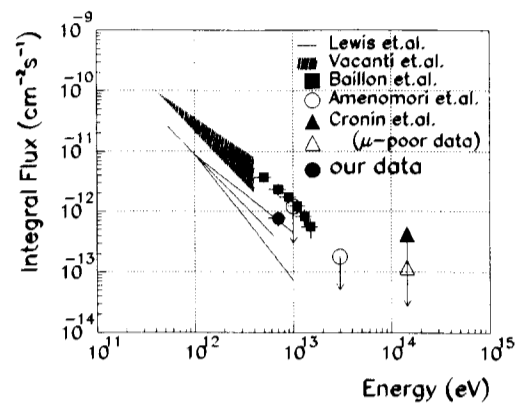


Figure 3: The integral flux of the present observation for γ -rays from the Crab pulsar/nebula. The previous and revised spectra of the Whipple group, the Themistocle data, and the upper limits of the flux at greater than 10 TeV are also presented.